The Equation of State of Dense Matter and Neutron Star Observations

Andrew W. Steiner (UTK/ORNL)

July 20, 2016

Outline

- RMF, Hyperons, Bose condensates
- Gibbs phase rules
- Surface tension
- NS Cooling and pairing
- LIGO
- r-modes
- NS crust
- Pulsar glitches

Covariant mean-field theory

- Walecka model:

$$\mathcal{L} = \bar{\psi}_i \left(i\partial\!\!\!/ - m_i + g_\sigma \sigma - g_\omega \omega\!\!\!/ - \frac{g_\rho}{2} \vec{\rho\!\!\!/} \cdot \vec{\tau} \right) \psi_i$$

$$+ \frac{1}{2} (\partial^\mu \sigma) (\partial_\mu \sigma) - \frac{1}{2} m_\sigma^2 \sigma^2 - \frac{bM}{3} (g_\sigma \sigma)^3 - \frac{c}{4} (g_\sigma \sigma)^4$$

$$+ \frac{1}{2} m_\omega^2 \omega^\mu \omega_\mu + \frac{1}{2} m_\rho^2 \rho^\mu \rho_\mu - \frac{1}{4} f_{\mu\nu} f^{\mu\nu} - \frac{1}{4} \vec{B}_{\mu\nu} \vec{B}^{\mu\nu}$$

Serot and Walecka (1997)

- Mean-field approximation; Dirac equation for nucleons and meson field equations
- Relativistic, so in principle can go to higher densities
- Spin-orbit force appears more naturally
- No problem with $c_s^2 > c$
- In this form, limited control of symmetry energy
- Natural generalization to include hyperons

Hyperons

- Appear when, e.g.
  $\mu_\Lambda(n_B, n_{\Lambda=0}) > \mu_n(n_B)$ or
  $\mu_{\Sigma^-}(n_B, n_{\Sigma^-=0}) > \mu_n(n_B) + \mu_e(n_B)$

- Hyperons decrease the pressure (less degeneracy)
- Binding energy of Λ in nuclear matter ~ 30 MeV
- Nucleons only models imply μ_n ~ 1600 MeV in the core
- Density-functional, Brueckner, or Walecka-type models
- "Hyperon problem" - 2 $M_\odot$ neutron star

TABLE III. Λ separation energies (in MeV) obtained using the two-body plus three-body hyperon-nucleon interaction with the set of parameters (II). The results already include the CSB contribution. In the last column are the expected B_Λ values. No experimental data for $A = 17, 18, 41, 49, 91$ exist. For ${}^{17}_{\Lambda}$O the reference separation energy is a semiempirical value. For $A = 41, 49, 91$ the experimental hyperon binding energies are those of the nearest hypernuclei ${}^{40}_{\Lambda}$Ca, ${}^{51}_{\Lambda}$V, and ${}^{89}_{\Lambda}$Y respectively.

System	AFDMC B_Λ	Expt. B_Λ
${}^{3}_{\Lambda}$H	−1.22(15)	0.13(5) [12]
${}^{4}_{\Lambda}$H	0.95(9)	2.04(4) [12]
${}^{4}_{\Lambda}$He	1.22(9)	2.39(3) [12]
${}^{5}_{\Lambda}$He	3.22(14)	3.12(2) [12]
${}^{6}_{\Lambda}$He	4.76(20)	4.25(10) [12]
${}^{7}_{\Lambda}$He	5.95(25)	5.68(28) [22]
${}^{13}_{\Lambda}$C	11.2(4)	11.69(12) [13]
${}^{16}_{\Lambda}$O	12.6(7)	12.42(41) [65]
${}^{17}_{\Lambda}$O	12.4(6)	13.0(4) [31]
${}^{18}_{\Lambda}$O	12.7(9)	
${}^{41}_{\Lambda}$Ca	19(4)	18.7(1.1) [14]
${}^{49}_{\Lambda}$Ca	20(5)	19.97(13) [66]
${}^{91}_{\Lambda}$Zr	21(9)	23.11(10) [66]

Boson condensates

- Equilibrium: $\mu_{\pi^-} = \mu_e$
- π^- and K^- condensates most common
- Decrease electron pressure and maximum mass
- Models based on chiral symmetry
  Kaplan and Nelson (1986)
- There is also π^0 condensation implicitly inside Akmal et al. (1998)
- Appear less likely than hyperons.
- Analogous excitations may also appear in superconducting quarks
  Bedaque and Schafer (2002)

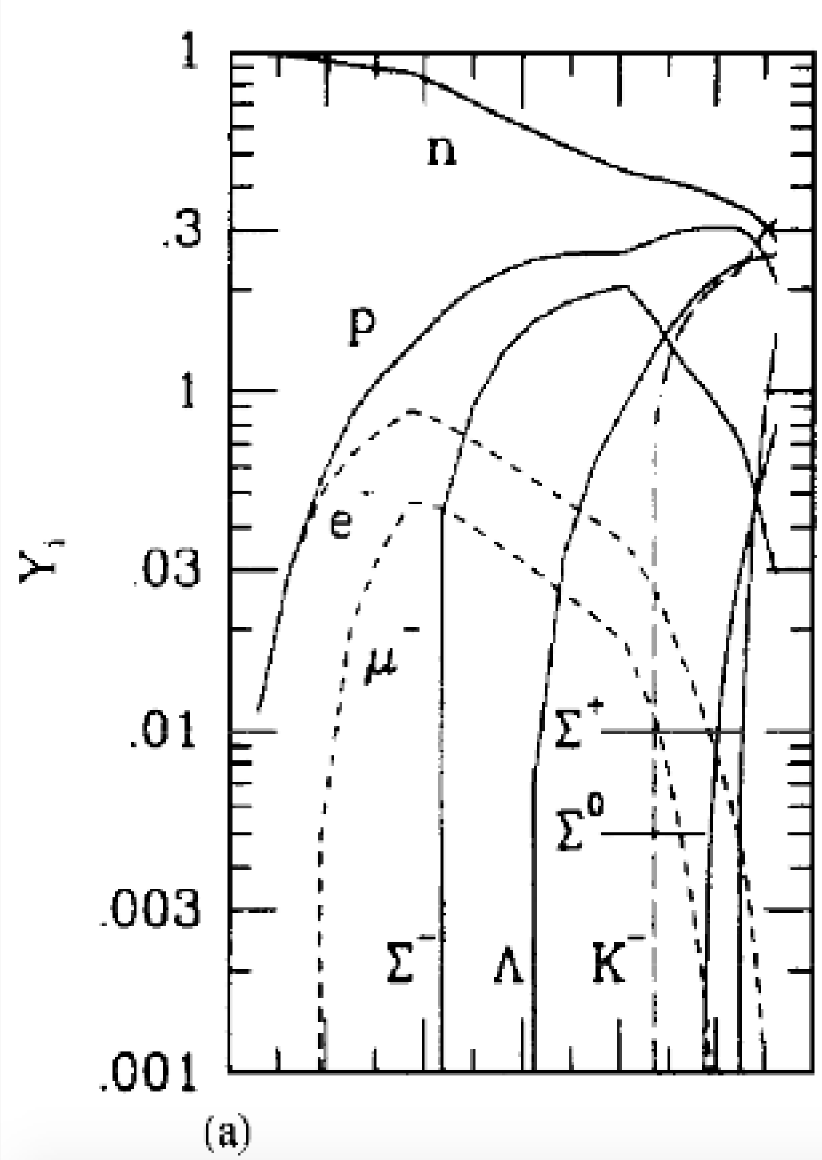

Prakash et al. (1997)

Gibbs Phase Construction

- Transition at a surface: mechanical $P_1 = P_2$, chemical $\mu_{i,1} = \mu_{i,2}$, and thermal equilibrium, $T_1 = T_2$
- A mixture of the two phases: volume fraction of the low-density phase, χ
- Local charge neutrality
  Glendenning (1992), Müller and Serot (1995)

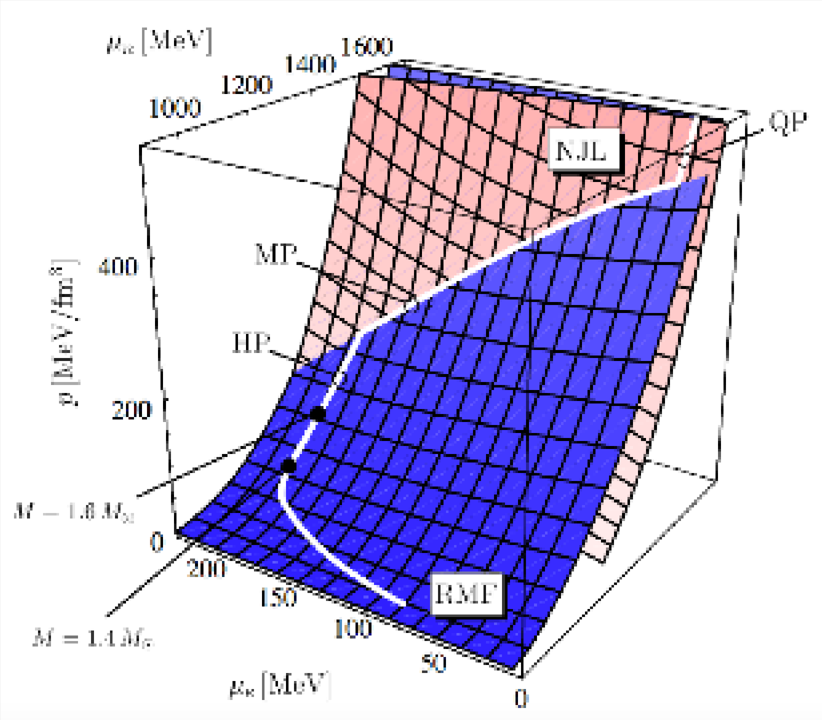

Schertler et al. (1999)

$$n_Q = 0 = \chi n_{Q,\mathrm{low}} + (1-\chi) n_{Q,\mathrm{high}}$$

$$n_B = \chi n_{B,\mathrm{low}} + (1-\chi) n_{B,\mathrm{high}}$$

- Minimize "internal" energy density, $\varepsilon(s,n)$
- Minimize free energy density, $f(n,T)$
- Maximize pressure, $P(\mu,T)$

Surface energy

- Surface tension is surface energy per unit area, $\sigma = S/(4\pi r^2)$
- Quark spheres embedded in hadronic matter are analogous to nuclear matter embedded in vacuum
- Sharp transition is limit of large surface tension
- Gibbs phase transition is often computed with zero surface tension
- We can compute surface and curvature energies with Thomas-Fermi or with Hartree-Fock
  Boguta and Bodmer (1977)

Divining the Core

- Hadrons and quarks can provide the same pressure
- Thus radii (sensitive only to the pressure) cannot determine the composition

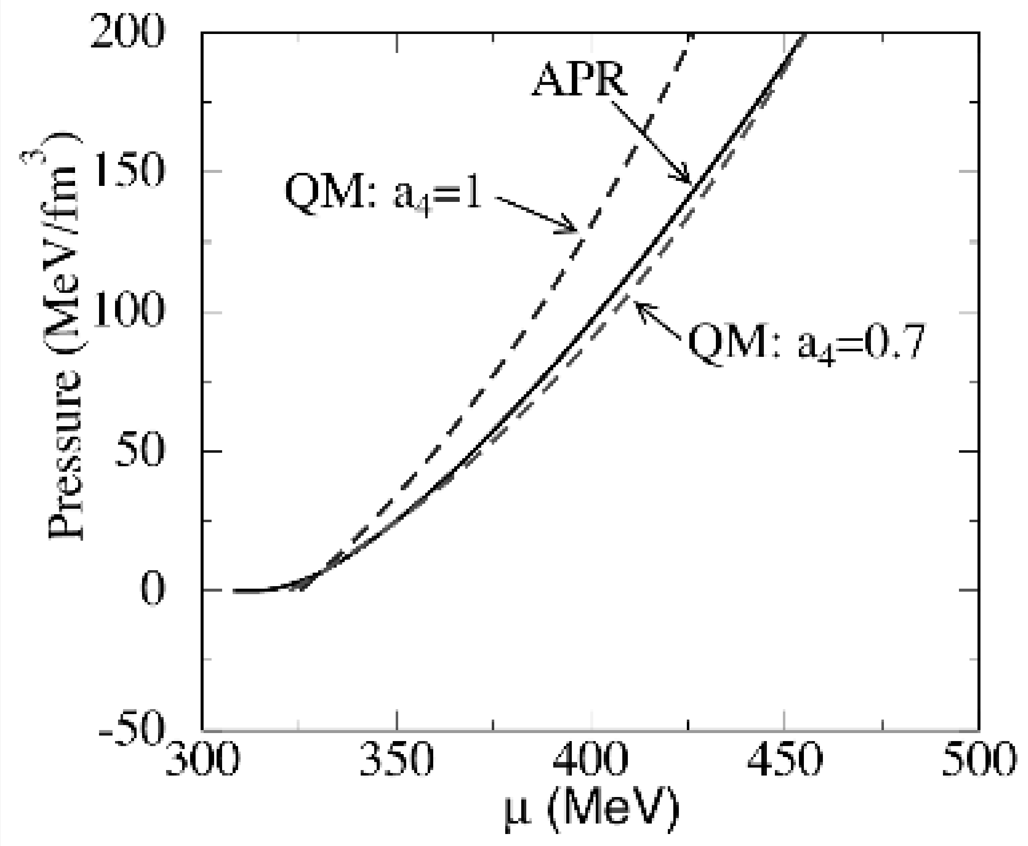

Alford et al. (2005)

- However! Hadrons and quarks often have different transport properties
    - Thermal and electrical conductivities
    - Shear and bulk viscosity, shear modulus
    - Neutrino and photon transport

Thermal Emission from Isolated Neutron Stars

- After ~ 10 years, the star is isothermal ⇒ one temperature = T

$$C_V \frac{dT}{dt} = L_\nu + L_\gamma\,, \quad L_\gamma \sim T^{2+4a}\,, \quad L_\nu \sim T^8\,[n+n \rightarrow n+p+e+\nu]\,, \quad C_V \sim CT$$

- Age assumed from spin-down age or associated with a supernova remnant

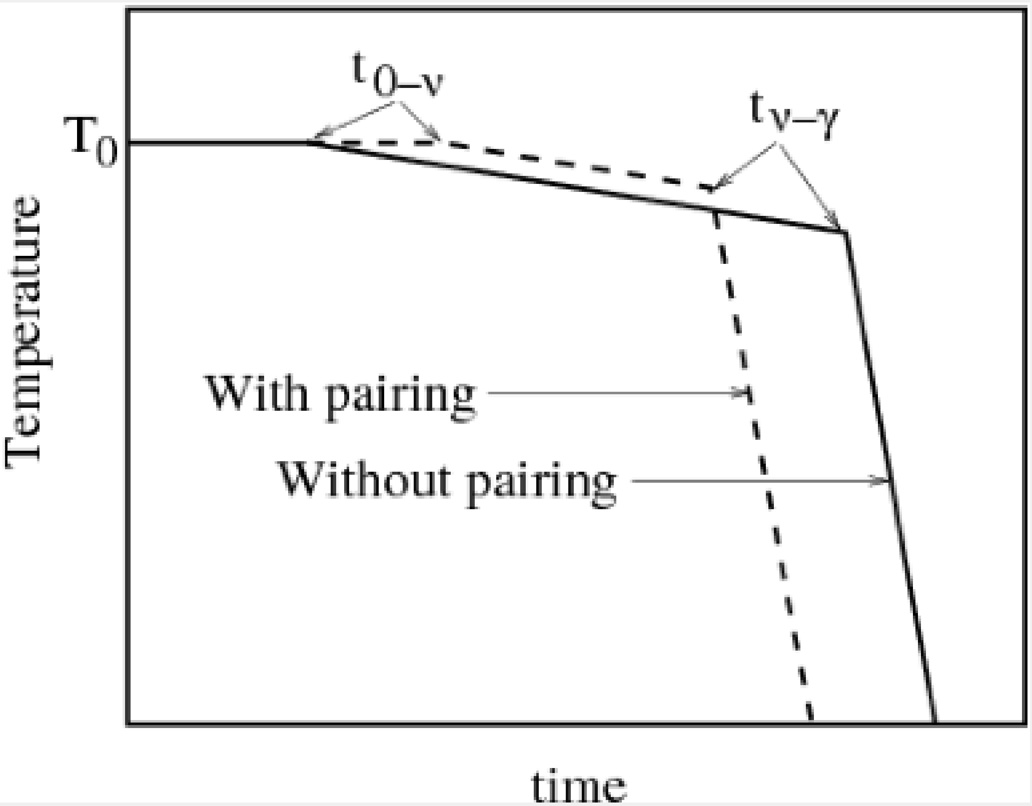

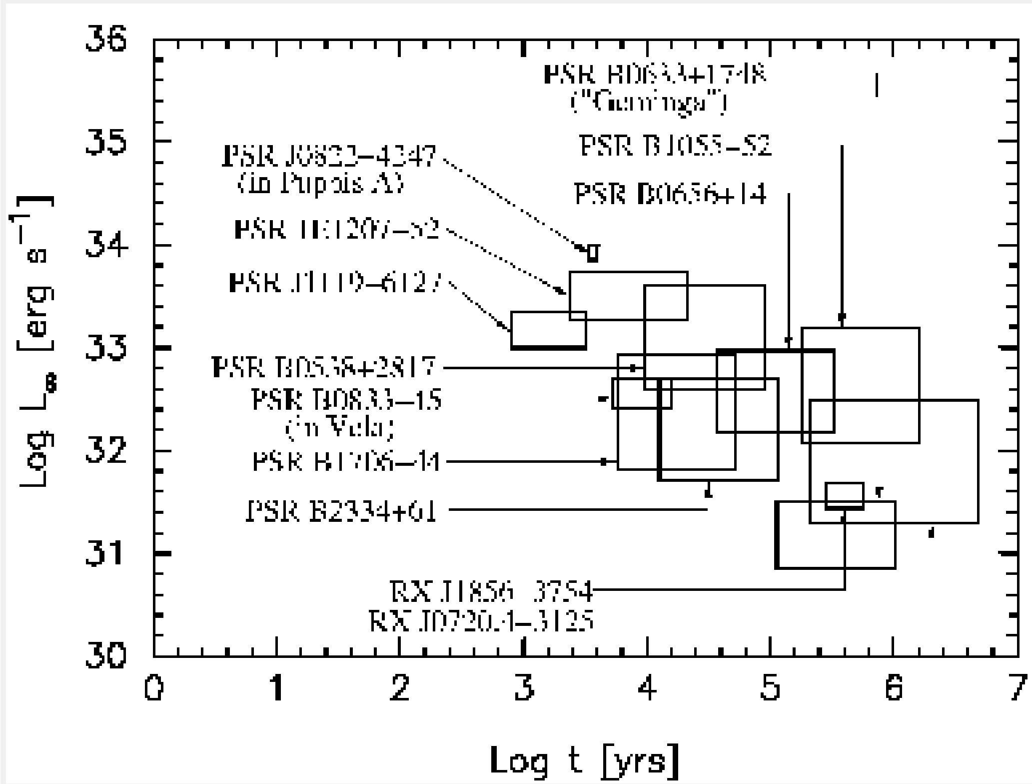

Page, et al (2004)

Page, et al (2009)

Table 21.1 A sample of neutrino emission processes. T_9 is temperature T in units of 10^9 K and the R's are control factors to include the suppressing effects of pairing (see Section 21.4.3).

Name	Process	Emissivity erg cm^{-3} s^{-1}	Efficiency
Modified Urca (neutron branch)	$\begin{cases} n+n' \to p+n'+e^- +\bar{\nu}_e \\ p+n'+e^- \to n+n'+\nu_e \end{cases}$	$\sim 2\times 10^{21} R T_9^8$	Slow
Modified Urca (proton branch)	$\begin{cases} n+p' \to p+p'+e^- +\bar{\nu}_e \\ p+p'+e^- \to n+p'+\nu_e \end{cases}$	$\sim 10^{21} R T_9^8$	Slow
Bremsstrahlung	$\begin{cases} n+n' \to n+n'+\nu+\bar{\nu} \\ n+p \to n+p+\nu+\bar{\nu} \\ p+p' \to p+p'+\nu+\bar{\nu} \end{cases}$	$\sim 10^{19} R T_9^8$	Slow
Cooper pair	$\begin{cases} n+n \to [nn]+\nu+\bar{\nu} \\ p+p \to [pp]+\nu+\bar{\nu} \end{cases}$	$\sim 5\times 10^{21} R T_9^7$ $\sim 5\times 10^{19} R T_9^7$	Medium
Direct Urca (nucleons)	$\begin{cases} n \to p+e^- +\bar{\nu}_e \\ p+e^- \to n+\nu_e \end{cases}$	$\sim 10^{27} R T_9^6$	Fast
Direct Urca (Λ hyperons)	$\begin{cases} \Lambda \to p+e^- +\bar{\nu}_e \\ p+e^- \to \Lambda+\nu_e \end{cases}$	$\sim 10^{27} R T_9^6$	Fast

Page et al. (2014)

Superfluidity

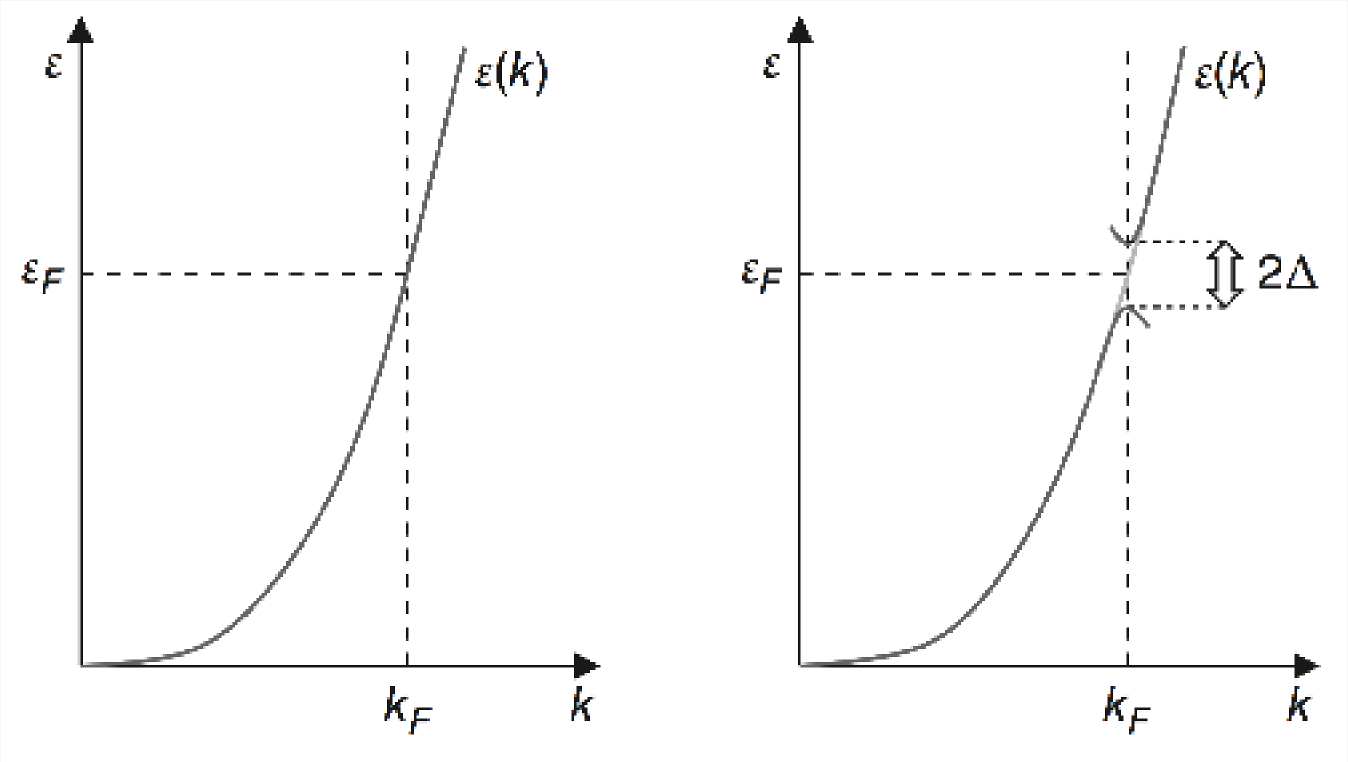

Page et al. (2014)

- Fermions which experience an attractive interaction become superfluid
- When they are charged ⇒ superconducting
- The origin of the exotic transport is the presence of an energy gap
- Near the Fermi surface, system gains energy by forming a Cooper pair
- Singlet ($^1S_0$) pairing requires the participants have nearly the same momenta
- Thus unusual to have one species pair with another
- Dramatic effect on specific heat

Neutron Star Superfluidity

Page et al. (2014)

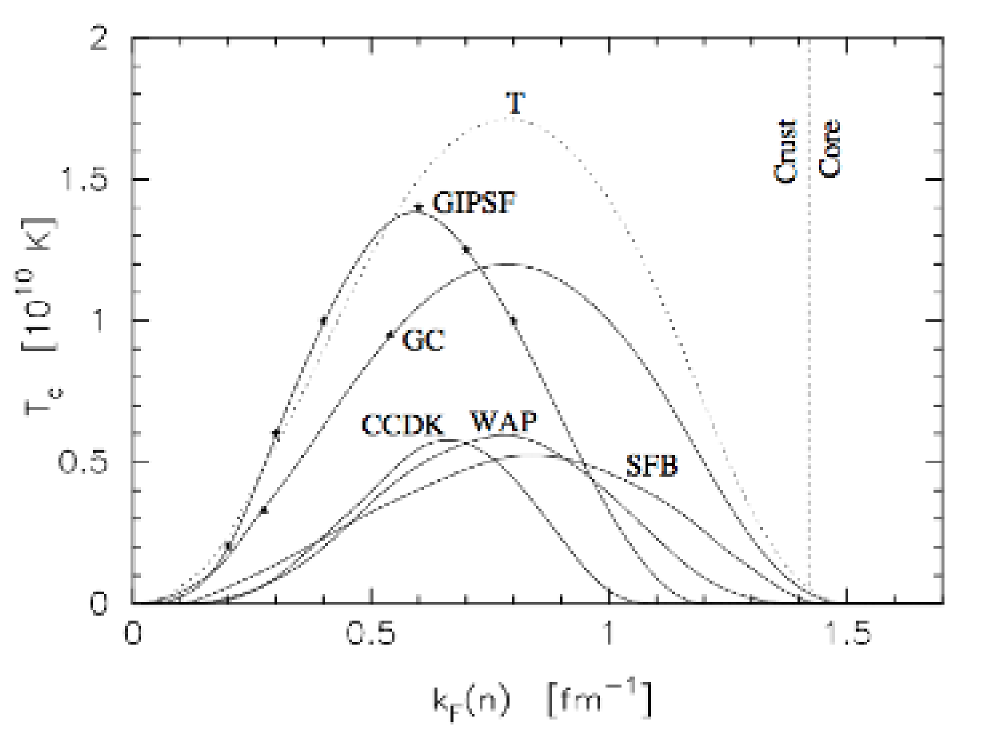

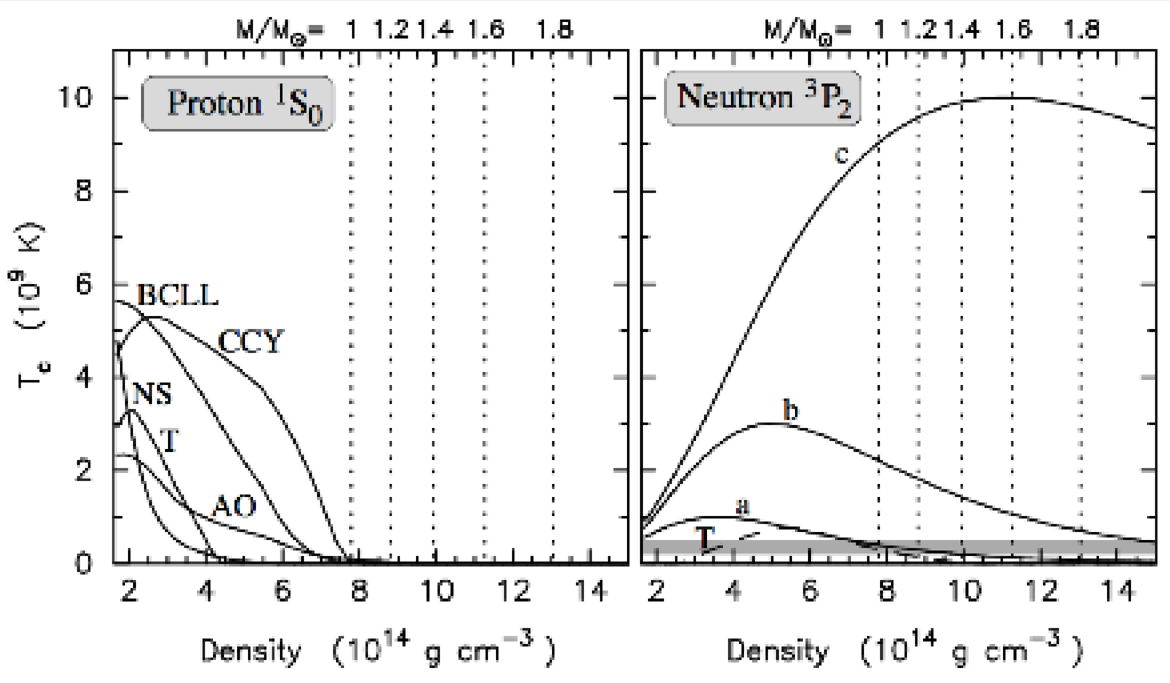

- $^1S_0$ gap increases with increasing density, but drops off at higher densities because of n-n repulsion
- Superfluidity can block cooling processes
- ...but it opens up new ways of cooling

Pair-formation emissivity

- Neutrons and protons are both paired in dense matter
- Neutrino pairs, broken by finite temperature, can reform
- The pairing energy can be used to generate a neutrino-antineutrino pair
- Very efficient cooling when kT ~ gap energy

Flowers et al. (1976), Leinson and Perez (2006)

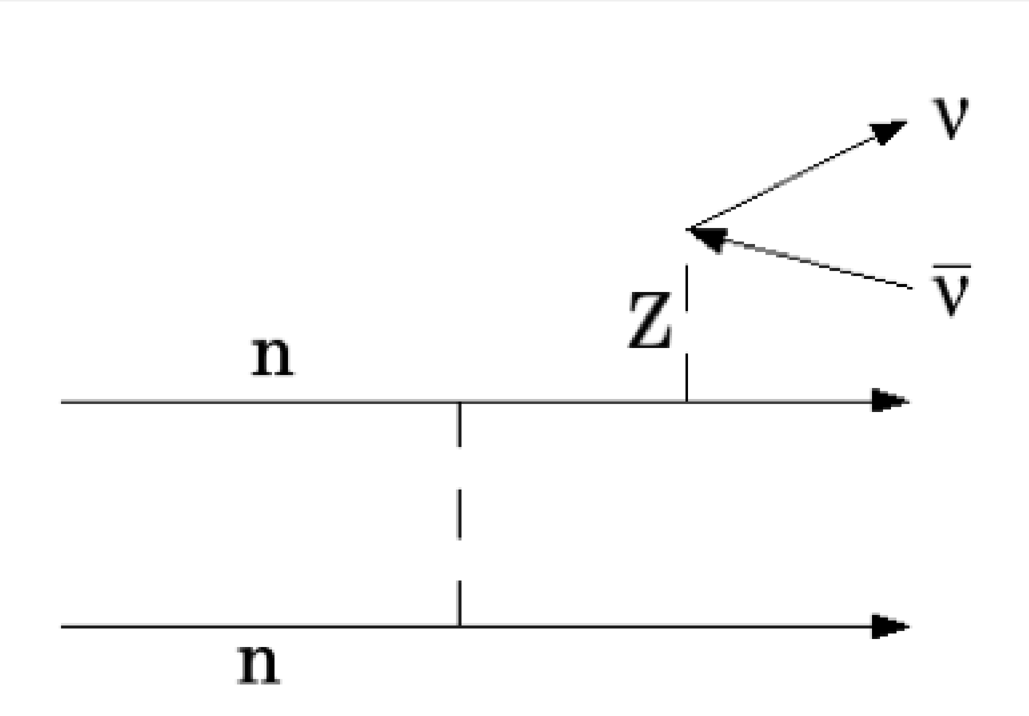

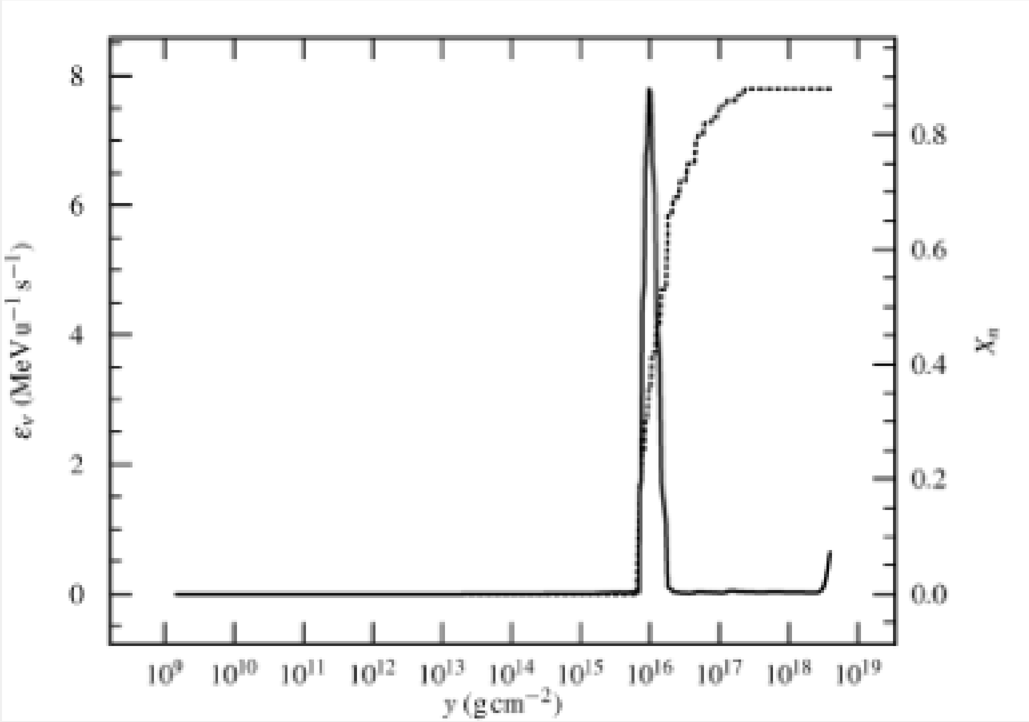

Cooper pair emissivity in the crust from Ed Brown

Detecting Neutron Star Superfluidity

- Neutron star in Cas A cooling very quickly
- The large slope is only well reproduced by the neutron triplet superfluid transition and associated emissivity
- Cas A requires a very particular triplet gap $\Delta(T=0) \propto T_C$

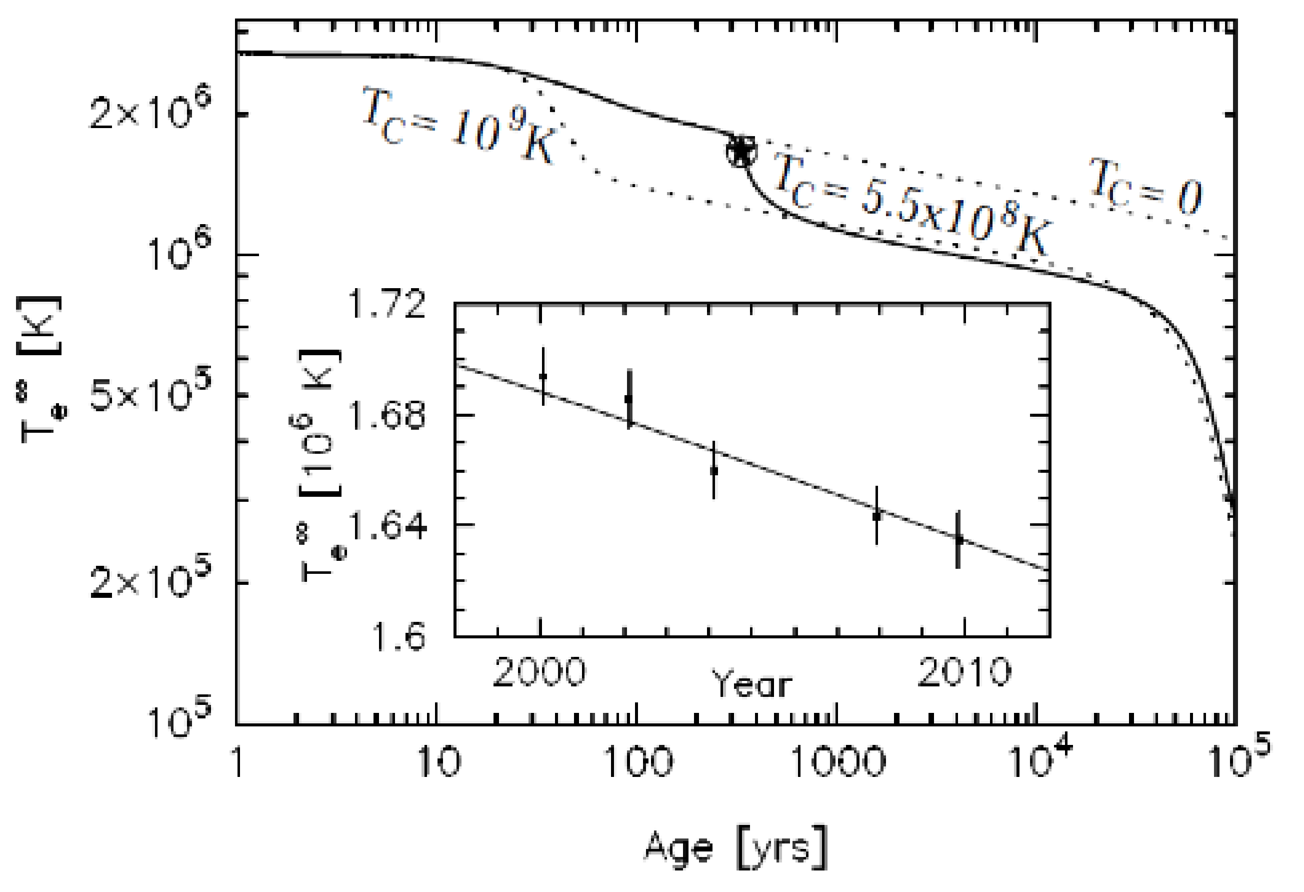

Page, et al. (2011)

Neutron Star Tidal Deformabilities

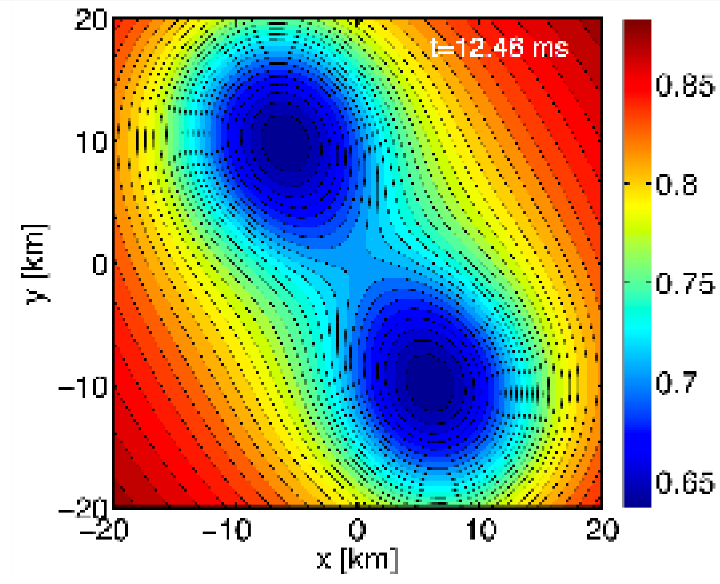

[Bauswein et al. (2016)](#)

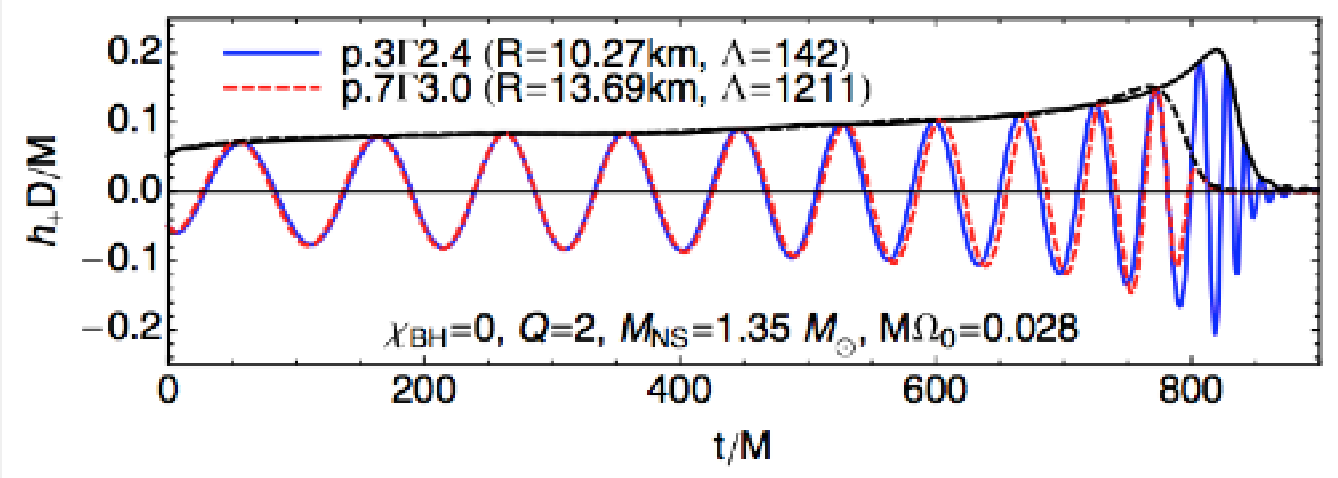

[Lackey et al. (2014)](#)

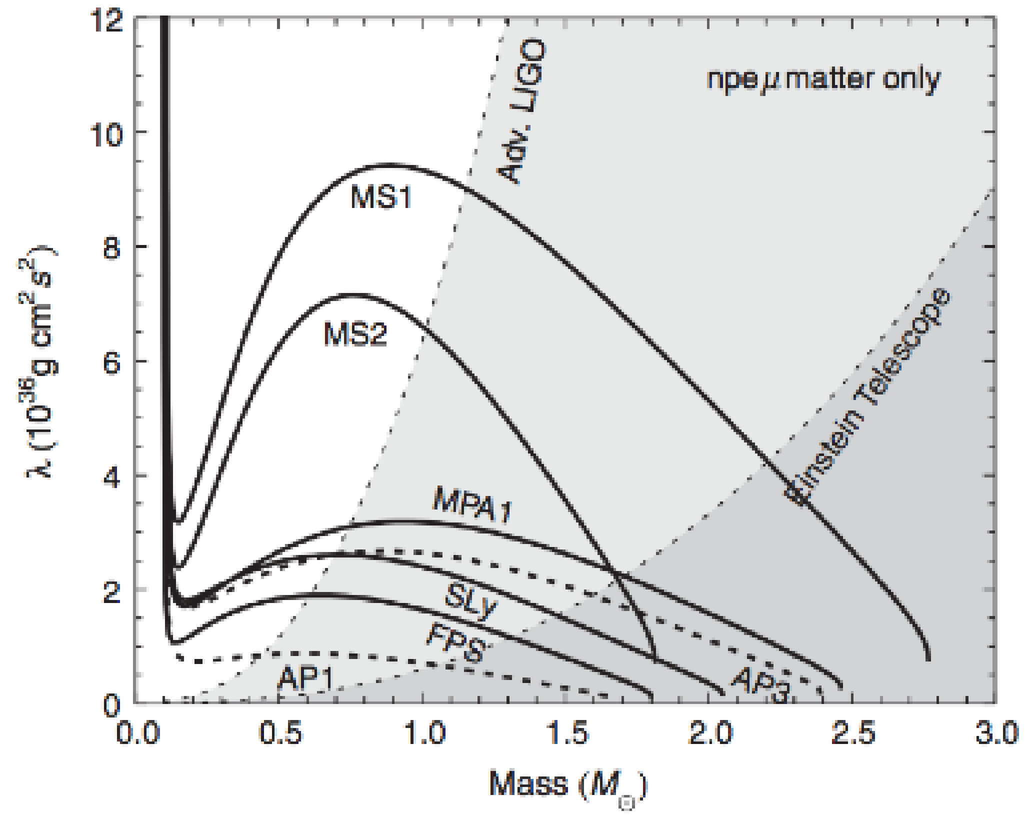

[Hinderer et al. (2010)](#)

- Gravitational wave signal from an NS merger measures tidal deformability λ
- Point masses early on; deformation near 400 Hz
- Easier to detect larger tidal deformations
- Nearly equivalent to a radius measurement

I and λ results

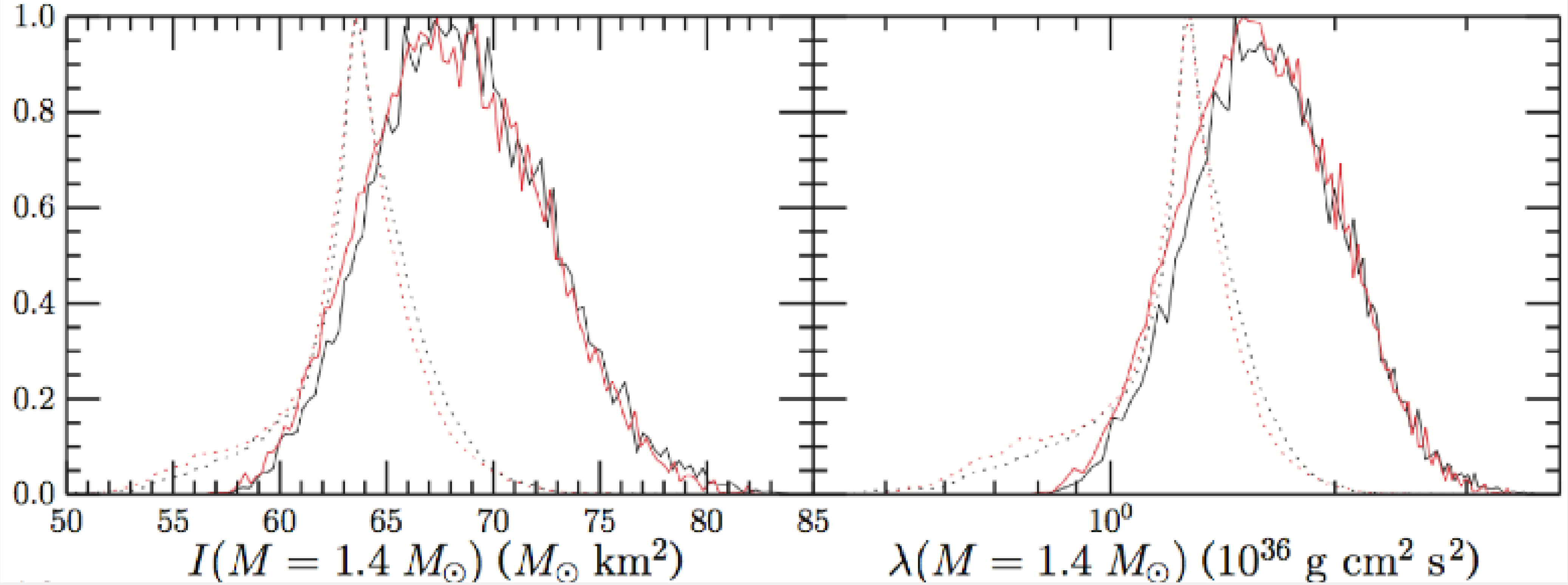

`Steiner et al. (2015)

- Predict moments of inertia and tidal deformabilities
- Tidal deformability is like a tidal polarizability for gravitational fields
- Potentially exciting comparison with LIGO observations
- Note again the strong model dependence
- These plots do not include several astrophysical systematics

Post-Merger LIGO signal

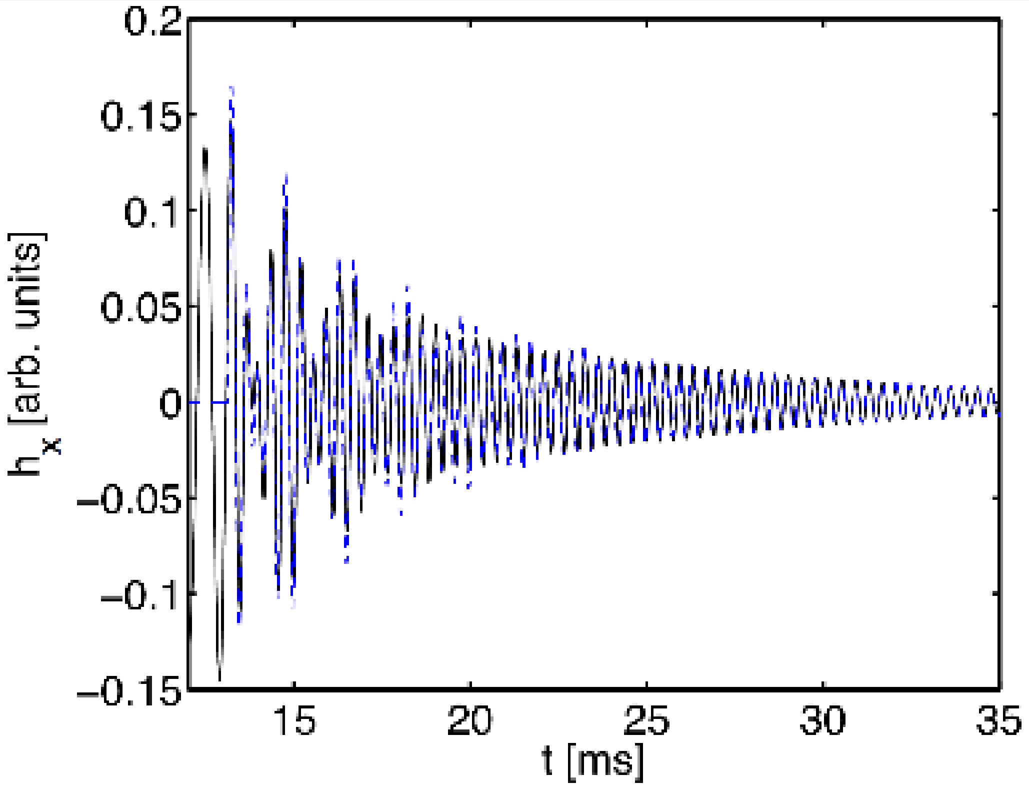

Bauswein et al. (2016)

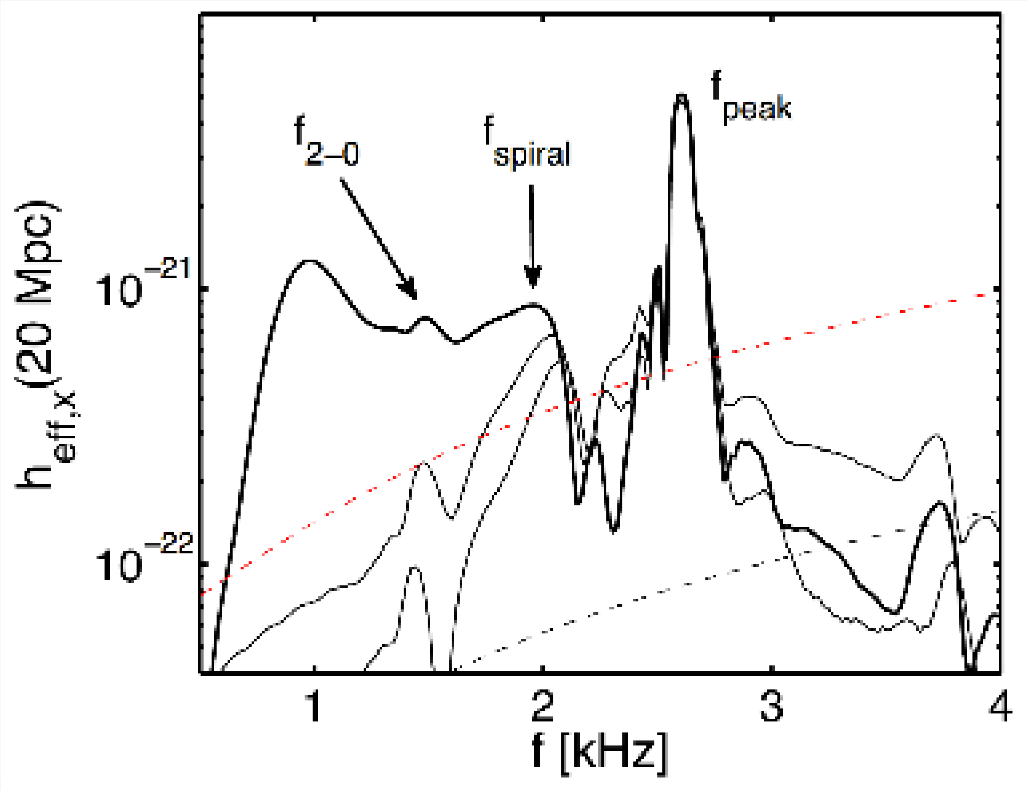

Bauswein et al. (2016)

- Post-merger signal is at higher frequency, thus more difficult to detect
- May provide information about the EOS and the NS structure, including radius, etc.

Neutron Star Spin

- Radio pulsations discovered by Jocelyn Bell Burnell and Antony Hewish in 1967
- "Pulsars" are neutron stars
- Pulsations not observed in all neutron stars
- Fastest observed neutron star spin, 716 Hz
- Magnetic dipole radiation, age ~ $P/\dot{P}$
- How does one obtain the maximum frequency?

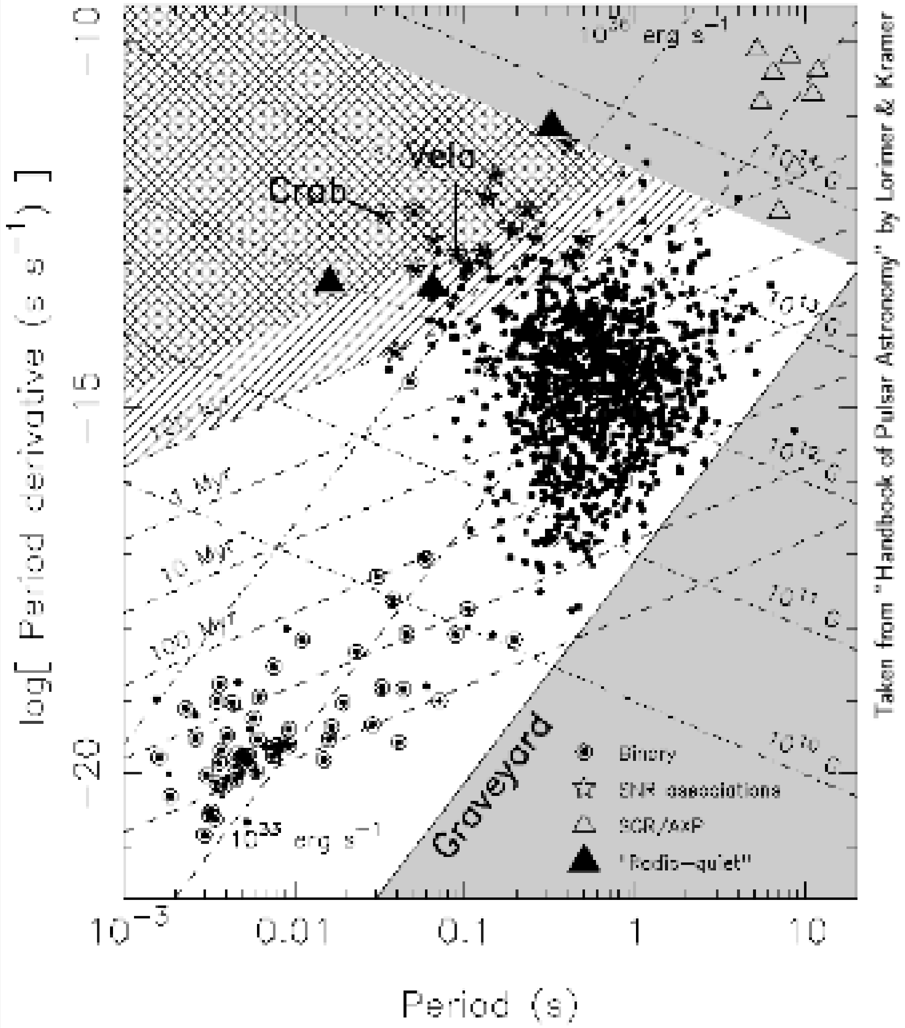

$$f_{\max} \approx 1\,\mathrm{kHz}\left(\frac{M}{M_\odot}\right)^{1/2}\left(\frac{R}{10\,\mathrm{km}}\right)^{-3/2}$$

Haensel et al. (2009)

Neutron star spin rates

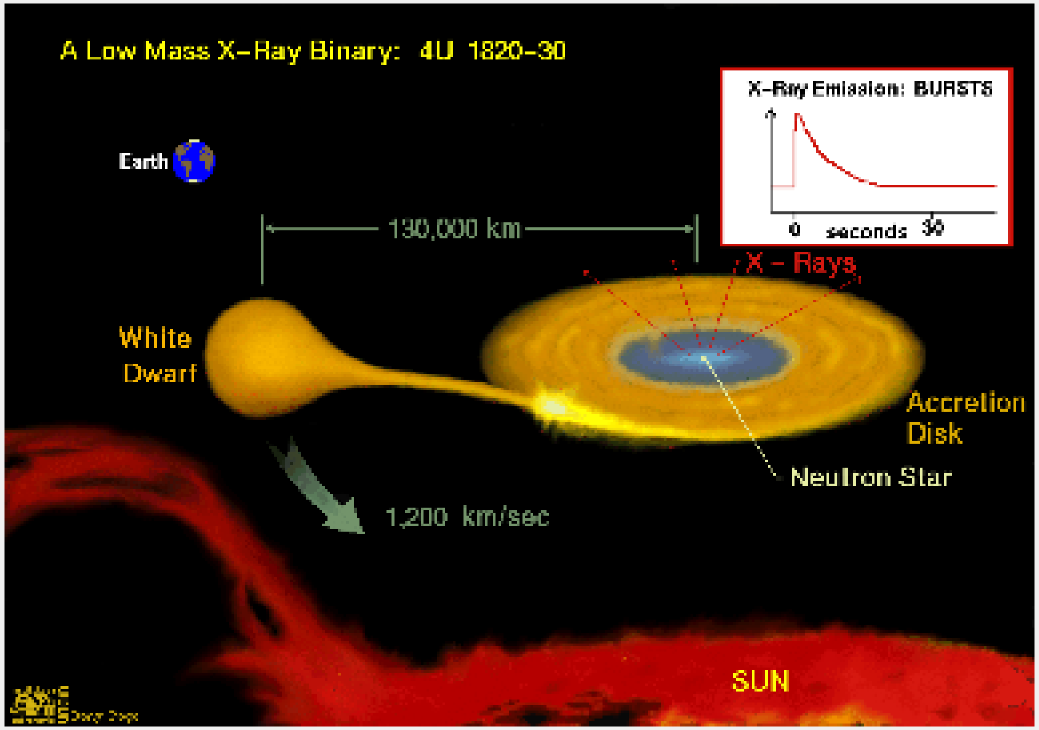

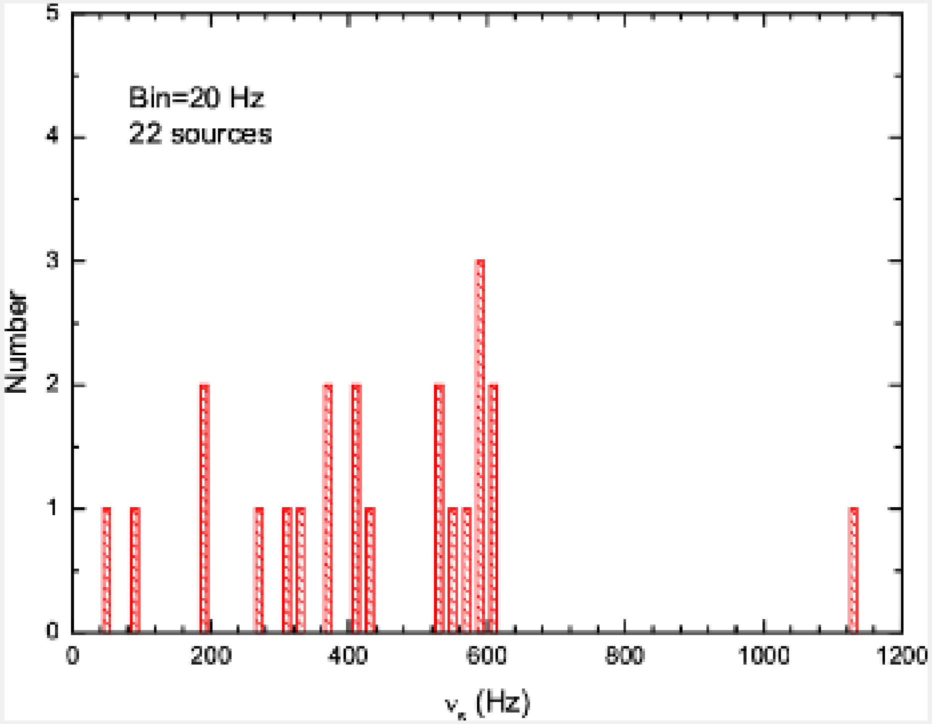

From D. Page

Yin, et al. (2007)

- Accretion expected to increase the spin rate
- Neutron stars don't spin as fast as they could
- Why? Possible answer: r-mode oscillations prevent faster spin rates

R-mode oscillations

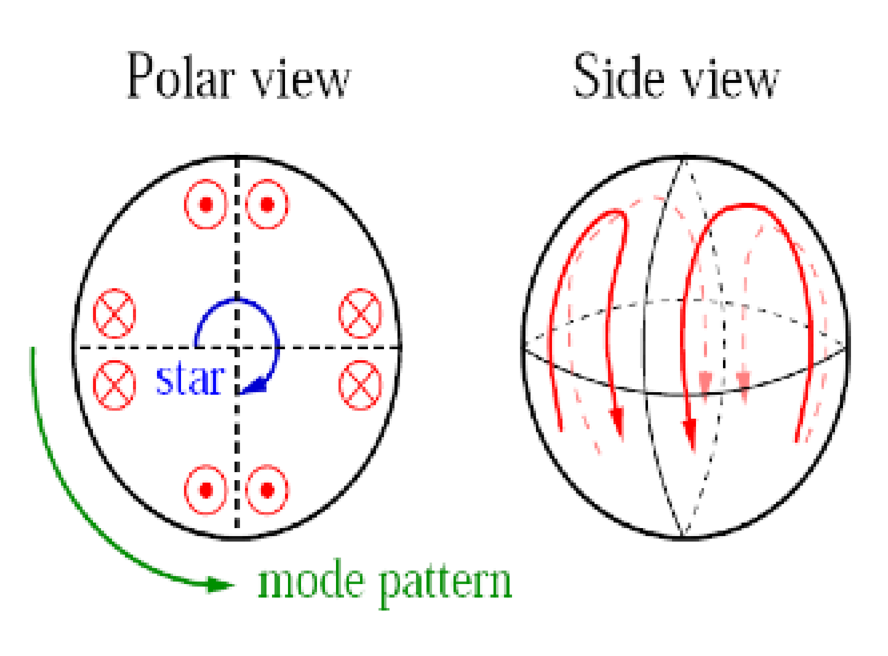

from M. Alford

- Toroidal fluid oscillations in rotating objects
- Oscillations grow because of GR, Chandresekhar-Friedman-Schutz instability

$$\omega = \omega_{\rm rot} - m\Omega = \left[\frac{2}{m(m+1)} - 1\right]\Omega$$

- Result: The star loses energy to gravitational waves and slows down
- Damping mechanisms: viscosity (temperature dependent) and saturation
- r-modes may have been detected: Strohmayer and Mahmoodifar (2013)

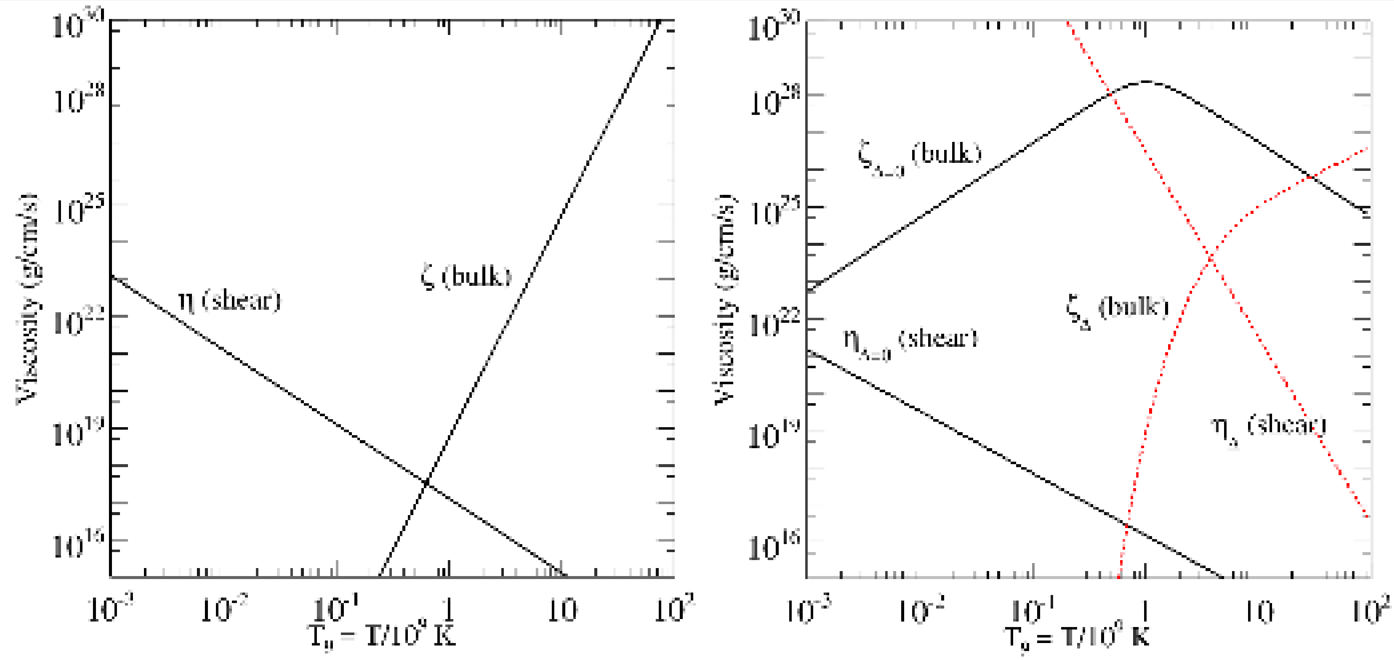

FIG. 2 (color online). The temperature dependence of the bulk and shear viscosity of neutron matter from Eqs. (21) and (22) (left panel) and that of ungapped and gapped quark matter from Eqs. (23) and (24) and Eqs. (25) and (29) respectively (right panel). For neutron matter, the energy density is chosen to be $1.5 \times 10^{-4} M_\odot/\mathrm{km}^3$ and $\kappa\Omega$ is fixed at 1000/s. For quark matter, the quark chemical potential is chosen to be 310 MeV, $m_s = 100$ MeV with $\Delta = 100$ MeV for CFL matter, and $\tau = 2\pi/\omega_r$ is fixed at 0.001 s.

[Jaikumar et al. (2008)]

- Viscosities of quark matter can be large

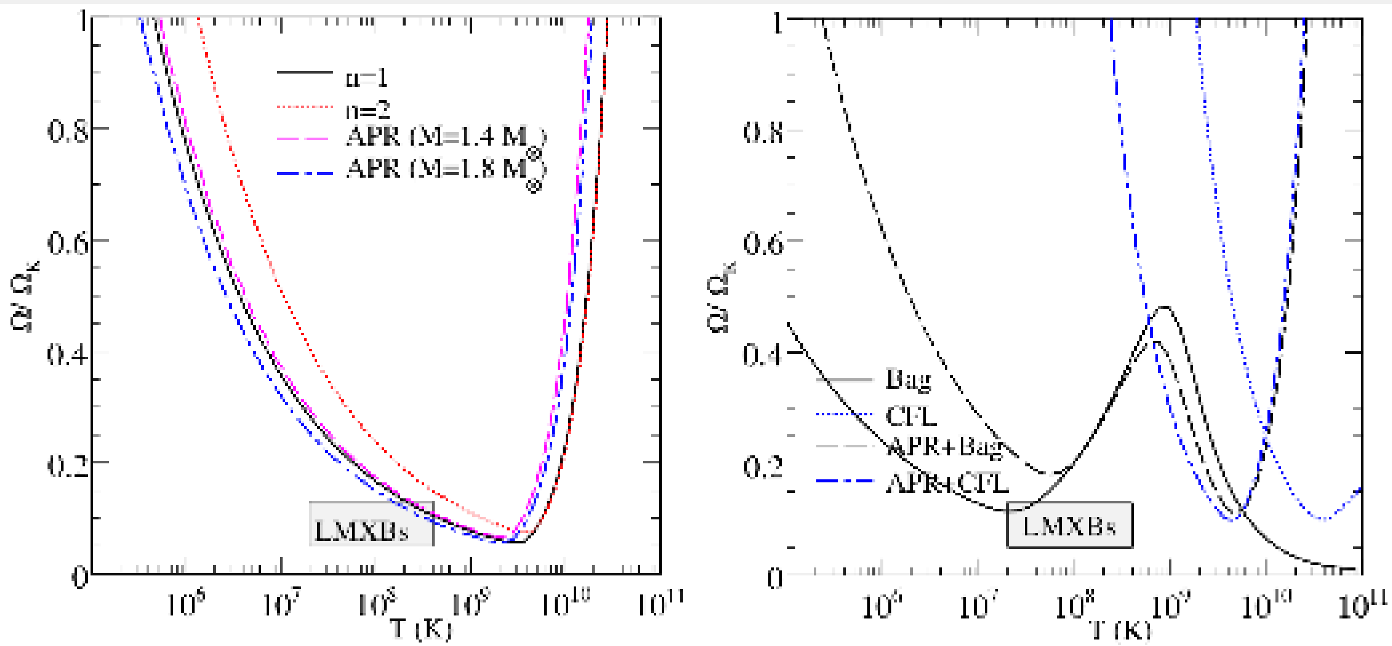

FIG. 4 (color online). The critical frequency Ω_c in units of Ω_K as a function of temperature for neutron stars, strange stars, and hybrid stars. For quark matter, we choose $m_s = 100$ MeV and $\Delta = 100$ MeV. The bag constant $B = 80$ MeV/fm^3 for strange stars, while $B = 110(150)$ MeV/fm^3 for hybrid stars with ungapped (CFL) quark matter. The box represents typical temperatures ($2 \times 10^{[illegible]} - 3 \times 10^{[illegible]}$ K) and rotation frequencies (300–700 Hz) of the majority of observed LMXBs assuming $\Omega_K = 5500$ Hz.

[Jaikumar et al. (2008)]

- Curves are maximum spin rate, so r-modes cannot cause spin-down
- More recent work finds extra viscosity [Alford and Schwenzer (2014)]

The Neutron Star Crust

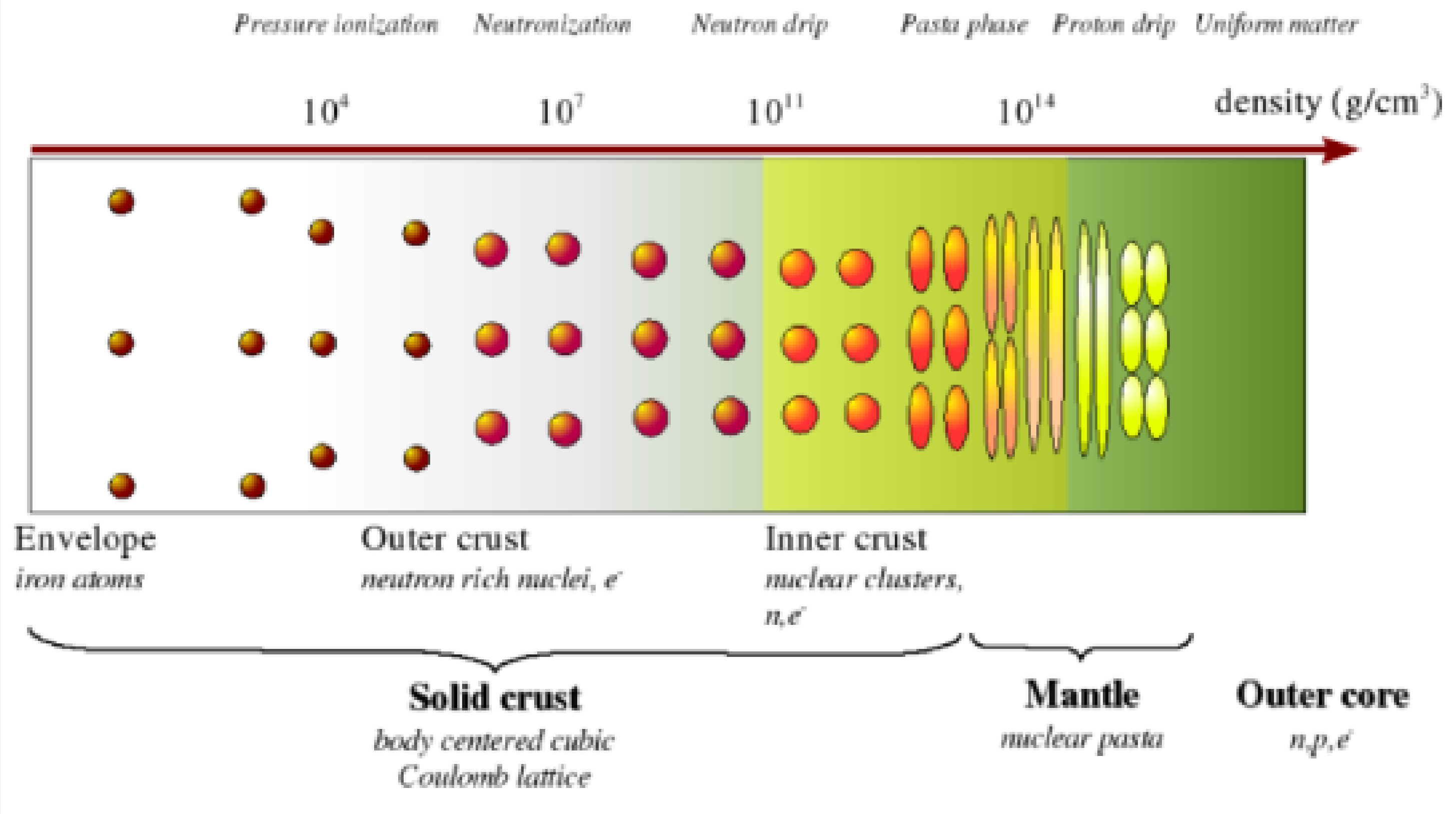

Chamel (2008)

- Nuclei → nuclei + neutrons → core (n, p, and e fluid)

Remember:

$$E(Z,N) = -BA + E_{\rm surf}A^{2/3} + CZ^2A^{-1/3} + S\frac{(N-Z)^2}{A}$$

- Coulomb modified at high density by lattice corrections